Application of the Low Frequency Raman Spectroscopy for Studying Ultra-High Molecular Weight Polyethylenes

Pavel Pakhomov,[*1] *Svetlana Khizhnyak,*[1] *Vladimir Galitsyn,*[2] *Ekaterina Rogova,*[2] *Brigitta Hartmann,*[3] *Alexandre Tshmel*[4]

Summary: In the frequency range below ~150 cm^{-1}, the longitudinal acoustic modes (LAM) localized along straight chain segments (SCS) of macromolecules emerge in the Raman spectra of linear semicrystalline polymers. The LAM frequency is inversely proportional to the SCS length; therefore, the LAM band contour reflects the SCS length distribution in a sample. The opportunities given one by the low-frequency Raman spectroscopy for studying the ordered structures in polyethylene are demonstrated and discussed. The illustrating material consists of both previously published and original data on nucleation and transformation of the ensemble of SCS in powder-like, gelled, and drawn ultra-high molecular weight polyethylene.

Keywords: gels; low-frequency raman spectroscopy; oriented fibers; reactor powders; ultra-high molecular weight polyethylene

Introduction

The low-frequency Raman scattering from localized acoustic vibrations in linear semicrystalline polymers (polyethylene, polypropylene, polyoxymethylene, etc.) allows one to determine the length of straight chains segments (SCS) situated both in amorphous and crystalline regions. These accordion-like, longitudinal acoustic modes (LAM) manifest themselves as Raman bands in the frequency range below 150 cm^{-1}.[1–2] The LAM peak frequency is inversely proportional to the SCS mean length, and its intensity is proportional to the number of SCS per unit volume in the polymer.

The LAM parameters contain important information on the molecular ordering in linear polymers. In this paper we shall discuss some applications of the low-frequency Raman spectroscopy in polymer studies. The capacity of this technique will be demonstrated using the data obtained by our research group during the last decade. A particular attention is focused on the role of the ordered structures in mechanical properties of polymeric materials.

Principles of Technique

Ordered Phase in Polyethylene

The capabilities of the LAM-spectroscopy will be demonstrated as revealed from the studies of the ordered structures in samples of ultra-high molecular weight polyethylene (UHMWPE) (molecular weight is about 10^6) taken in different states, such as nascent powder, gel and oriented fiber.

The diversity of UHMWPE structures is specified, to a considerable degree, by the

[1] Physico-Chemistry Department, Tver' State University, Sadovy per.35, 170002 Tver', Russia
Fax: (007) 4822 411275;
E-mail: pavel.pakhomov@mail.ru
[2] Institute of Synthetic Fiber, Moscovskoe shosse. 170032 Tver', Russia
[3] Physico-Chemistry Department, University of Osnabrueck, Barbara str. 7, D49069 Osnabrueck, Germany
[4] Ioffe Physico-Technical Institute, Russian Academy of Sciences, Polytechnicheskaya 24,194021 St. Petersburg

space and length distributions of the long all-*trans* sequences, which compose ordered entities of various kind, such as folded chain crystals, extended chain crystals and bundles of straight chain segments of macromolecules, all of which could (co-)exist, as suggested, in species with a very different pre-history. The properties of the SCS ensemble are closely related with the morphological pattern of the given sample through the prevailing type of the crystallization process at the stage of polymerization and during subsequent processing.

The information on the ordered phase in semi-crystalline polymers is available from a number of experimental techniques, each of which has its advantages and restrictions. Basic characteristics of the crystalline phase are available from the differential scanning calorimetry (DSC) and the X-ray scattering data. The latter technique is sensitive only to more or less perfect crystallites, while the former method enables to detect both truly crystal entities, and partially ordered clusters of SCS. The IR spectroscopy distinguishes all-*trans* sequences but cannot determine their length if the number of *trans*-conformers exceeds 4 units. Finally, the LAM-spectroscopy detects all kinds of all-*trans* sequences independently on their structural localization in a polymeric material, that is in crystals, bundles of SCS, or in individual fashion, and gives one an opportunity to obtain the SCS-length distribution, which characterizes in a specific manner the properties of the collection of *all-trans* segments in the semi-crystalline polymer.

Light Scattering from Individual Straight Chains

In semi-crystalline polymers, longitudinal acoustic vibrations propagate along regular molecular segments like along the elastic rods. Owing to their efficient interaction with the light, these modes produce specific, highly polarized bands in the low-frequency Raman spectra (in the range 5–10 to 100–150 cm^{-1}). It should be stressed that the linearity of the chain is the necessary condition of the LAM propagation. Finally, the LAM are localized in individual macromolecules, and their frequency, in fact, does not depend substantially on the nature of the chain environment.

SCS Length Distribution

Generally, the length of regular sequence between chain-ends and/or defects (gauche-conformers, points of branching) is related with the LAM frequency as:

$$L = (2c\omega_L)^{-1} \times (E/\rho)^{1/2} \quad (1)$$

where c is the speed of light; ρ is the density, and E is the Young's modulus. The frequency of the LAM band maximum allows one to calculate with the most probable length of the straight segments the help of Eq. (2).

As far as each SCS of a given length has its specific LAM frequency, the whole LAM band profile reflects the contribution of the SCS of different lengths to the Raman intensity, or, in other words, the average-number SCS length distribution. The position of the LAM band maximum characterizes, correspondingly, the length of the most numerous all-trans fraction in a sample; as a rule, the this is close to the longitudinal size (fold period) of crystallites measured along the chain orientation. However, this estimate gives only an approximate value. Owing to the dependence of the distribution function F(L) not only on the number of oscillating SCS but also on the scattering efficiency of light and the population of vibrational energy levels, the original Raman spectrum is poor representative for aims of quantitative estimations, and F(L) must be computed using a procedure based on the relation[3]:

$$F(L) \propto n(\omega)\omega^2 I_{LAM}(\omega) \quad (2)$$

Here the function n(ω) characterizes the Boltzmann population of vibrational energy levels: n(ω) is equal to [1-exp(-hcω/kT)] or [exp(hcω/kT)-1] in dependence of the Stokes and anti-Stokes scattering, respectively (here, h is Plank's constant, k is Boltzmann's constant, and T is the absolute temperature). $I_{LAM}(\omega)$ is the

Raman intensity, I, corrected for the Rayleigh scattering that gives a parasitic addition to the experimentally measured value I. To exclude the contribution of the Rayleigh scattering, a background of the LAM spectrum in the vicinity of the central line must be approximated with an appropriate analytical function. As a rule, the Lorentzian is well applicable for fitting the central line.

The value of the distribution function F(L) calculated at a given L is proportional to the amount of the SCS with the length equal to L. These SCS could be situated both in crystallites and amorphous regions, as well as in the interfibrillar space, since the light scattering events of this kind are of one-dimensional character and not related to any three-dimensional structural units.

Raman signal from an oriented PE sample in the vicinity of the central line is a sum of the Rayleigh scattering and the LAM band intensity. To exclude the contribution of the former component, a portion of central line under the LAM spectrum is approximated with a Lorentz function. The difference between the experimental spectrum, $I(\omega)$, and the approximating Lorentzian, $I_{Lor}(\omega)$, is taken as the effective intensity I_{LAM} in Eq. (2); $I_{LAM}(\omega) = I(\omega) - I_{Lor}(\omega)$. A graphical illustration of this mode of the Raman data processing one can see in Figure 1.

Non-Oriented Polymer

Gels

Gelled UHMWPE is a widely utilized raw substance that serves for manufacturing high-strength, high modulus fibers and films.[4] The mechanical properties of fibers depend, to some extent, on the molecular properties of gelled polymer, from which a fiber was formed. One of these properties is the capability of gels to form a tenuous spatial network of interconnected macromolecules, which would provide the mechanically stable structure of fiber obtained by thermal gel drawing. The role of entanglements in the physical gel network in semi-crystalline polymer could be played by microcrystallites,[5,6] therefore, the self-organizing processes in polymer solutions, such as straightening and regular packing of macromolecules, draw attention of specialists.

Studies of UHMWPE gels, which were carried out using the Raman (LAM) spectroscopy and the DSC method[7–10] confirmed the De Genes' conjecture that the entanglements in the molecular network in gels are built of folded crystals (lamellar microcrystallites). Figure 2a shows the low-frequency Raman spectra of a UHMWPE gelled in different solutions. One can see wide LAM bands in the

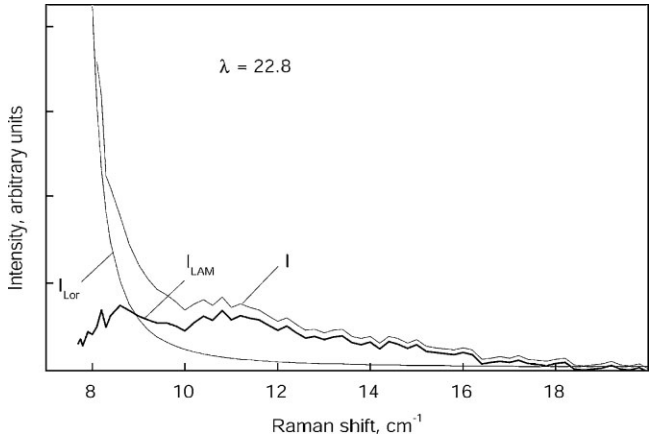

Figure 1.
An example of the spectroscopic data processing: the true LAM intensity results from the subtraction of the Lorentzian-fitted central line from the experimental spectrum.

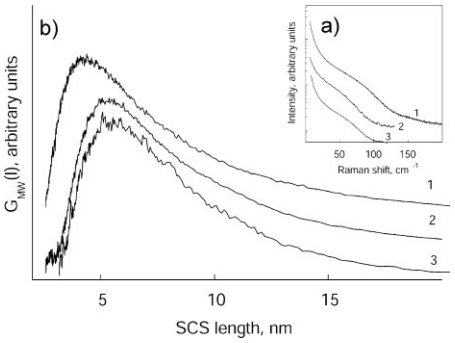

Figure 2.
Low-frequency Raman spectra (cut-ins) and calculated from them SCS length distributions (b) in the UHMWPE gelled in solutions in *p*-xylene (1), paraffin oil (2), and decaline (3). A logarithmic scale for the Raman intensity is used here, and in Figure 3 and Figure 9 in order to represent weak signals in detail.

range 40 to 100 cm^{-1}. This signalizes the presence of regular molecular segments in samples. The SCS length distributions calculated from these spectra are shown in Figure 2b. As it was mentioned above, the F(L) maxima positions indicate the lengths of the most probable SCS length in the sample (L_p). One can see that the L_p is sensitive to the solvent selected: the L_p in gels obtained from solutions in *p*-xylene, decaline and paraffin oil was equal to 3.7 nm, 5.0 nm, and 5.2 nm, respectively.

All Raman spectra presented in this work were obtained with a triple monochromator DILOR XY 800 equipped with a Spectra Physics 100 mW NdYVO4 laser (non-oriented samples) or with a triple monochromator Spex Model 1401 equipped with a 50 mW He-Ne laser (oriented samples).

On the other hand, it was found that the L_p depends, actually, neither on the solution concentration, nor on the polymer molecular weight (MW). The former fact points out that the SCS in gels are not isolated trans-sequences but involved into some crystalline entities, whose dimensions are determined by the thermodynamic conditions held during their forming. Therefore, one can accept that the L_p coincides with the mean thickness of microcrystallites.

The X-ray scattering study of the same samples[11] demonstrated that the lateral dimensions of crystalline entanglements were larger than longitudinal ones, and reached 18–20 nm.

Xerogels

The primary process in a series of procedures needed to obtain any final product from gelled polymer, such as highly oriented fiber, is the removal of solution. The dried gels (xerogels) are highly porous substances. In order to assess the transformation of the molecular network as a result of gel drying, the LAM spectra of the xerogels samples were recorded.

Figure 3 shows the function F(L) for a UHMWPE gel and its dried form. A pronounced asymmetry from the side of larger L evidences the distorted geometry of the principal planes of crystallites. Provided the solution removed, the L_p decreases from 5.1 down to 4.3 nm, the function F(L) becomes narrower and exhibits some bimodality. This means, first,

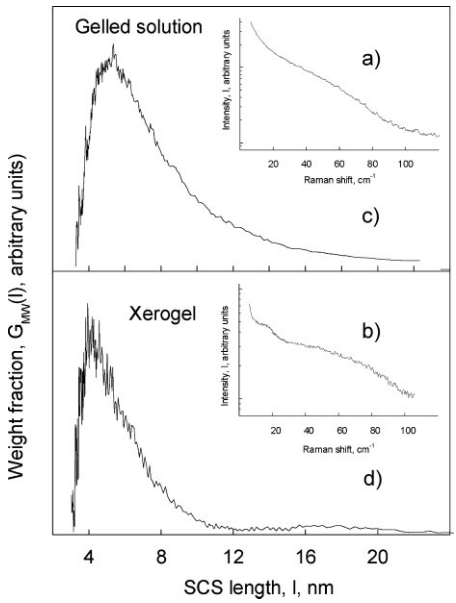

Figure 3.
Low-frequency Raman spectra (cut-ins) and calculated from them SCS length distribution function in UHMWPE gel and xerogel originated from gelled solution in paraffin oil.

smoothing of the crystallite surface as a result of folding of a part of SCS. Second, the appearance of an extra peak at ~17 nm points out the formation of some amount of SCS, whose lengths exceed significantly the longitudinal size of crystallites (L_K). Such dimension could be caused by the penetration of a certain amount of SCS into adjacent crystallites with forming regular sequences. A simple estimate shows that the isolated peak at 17 nm belong to the SCS that connect a series of three successive crystallites. This means that in consequence of the gel-to-xerogel transition, some SCS link adjacent crystallites with forming clusters (sandwich-like structures) consisting of 2-3 complanar lamellar crystals.

Oriented Polymer

The tenuous molecular network in gels is as flexible as individual macromolecular chains; at the same time, its entanglements are highly robust. Such network transforms readily into the oriented structure as a result of the extrusion or/and hot drawing of xerogels. The SCS length distributions in UHMWPE fibers differing in draw ratio (λ) are depicted in Figure 4. One can see that the oriented structure is characterized by the presence of quite long SCS, being the SCS length distribution dependent on the draw ratio. As a result of the λ increase, first, the maximum of the function F(L) shifts in direction of longer SCS, and, second, the length distribution becomes

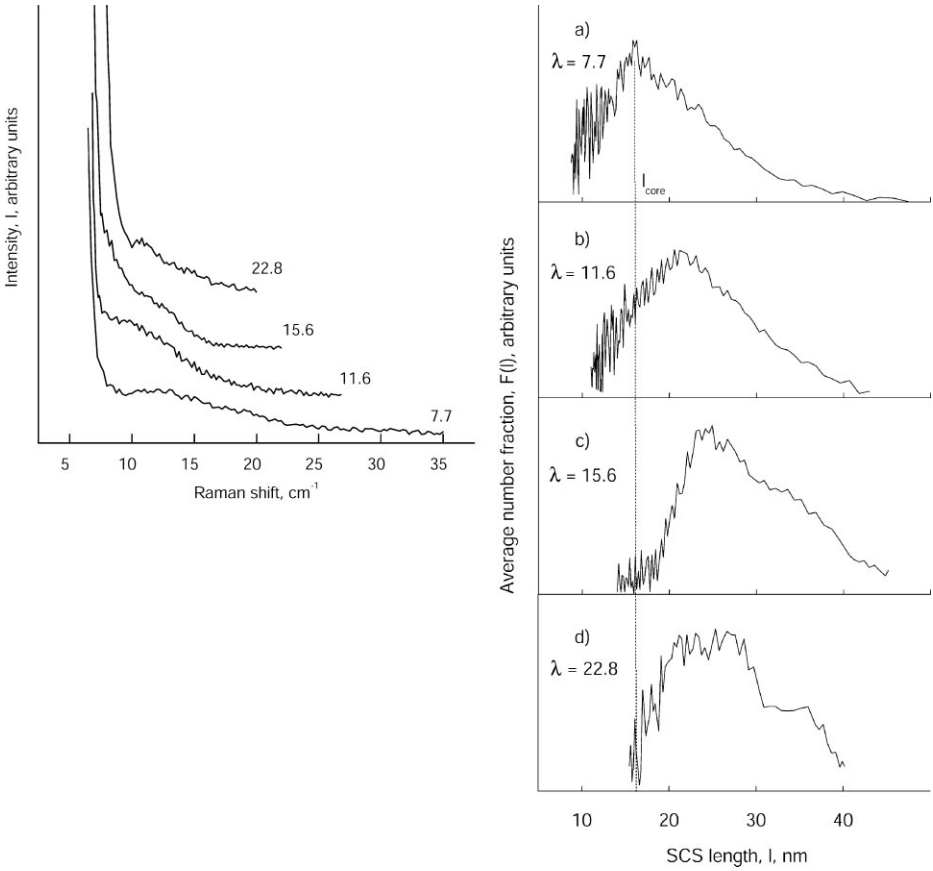

Figure 4.
Low-frequency Raman spectra in the range of the LAM bands (left) and calculated from them SCS length distributions in UHMWPE fibers with different draw ratios (right). Values λ are shown in figures.

asymmetric or bimodal. Generally, one can write:

$$L_{SCS} = L_K + L_{RAP}, \quad (3)$$

where L_K is the longitudinal size of crystallite, and L_{RAP} is the length of so called ''rigid amorphous phase'' that is a partially (longitudinally) ordered layer in the region between the crystalline phase and the truly amorphous (fully disordered) phase. In the weakly drawn $\lambda = 7.7$-sample, $L_{SCS} \approx L_K$ and $L_{RAP} \approx 0$, similarly the case of the gelled sample. It is well established[12] that the value of L_K does not depend on the fiber draw ratio at the given drawing temperature since it is determined by the thermodynamics of the chain folding process. Hence, one can conclude that the long-length shift of the F(L) maximum with the λ increase (Figure 4) is caused by the chain-fold straightening on the crystal surface with forming the RAP.

At $\lambda \geq 15.6$, the F(L) becomes bimodal (Figure 4c). The position of the second peak $L \approx 35$ nm is close to the value $2 \times L_K \approx 32$ nm, where $L_K \approx 16$ nm in the $\lambda = 7.7$-sample (Figure 4a). This means that the bimodal SCS distribution is related with the arising of taut-tie molecules, which connect a couple of adjacent crystallites. Interestingly, that when the RAP emerges in the oriented fiber, the fiber elastic modulus starts to grow (Figure 5). It should be stressed that the qualitative change in the SCS length distribution does not affect the quasi-linear increase of the Young's modulus at $\lambda > 7.7$ (Figure 5a). This interconnection between the Young's modulus and λ demonstrates that the transformation of the RAP into a set of taut-tie molecules does not disturb the ''morphological continuity'' of the drawing process.

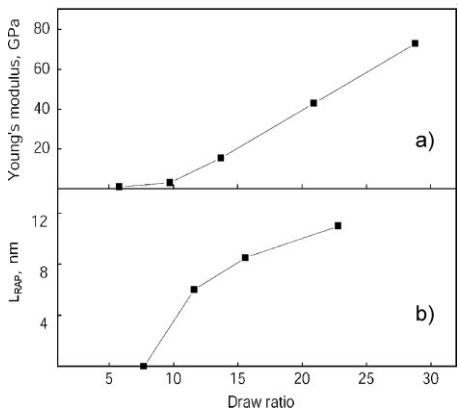

Figure 5.
Draw ratio dependence of Young's modulus (a) and RAP mean length (b) in UHMWPE fiber.

Thus, the expanding of the ''crystalline continuity'' along the fiber axis is caused by the chain unfolding on the surface of the lamellar crystallites. This process was firstly found by Galytsyn et al.[13] in the experiment on the stress relaxation under isothermal conditions. The appearance of the RAP phase in parallel with the growth of the Young's modulus supports the ''bridging model'' of the structure of highly oriented fiber, which was put forward by Ward et al.[14–15] to explain a paradoxical X-ray scattering experiment that demonstrated the crystallite longitudinal dimension exceeding the ''long period'' length. According to the bridging model, the ''long'' crystal entities composed of SCS could link the folded crystallites.

The bimodality in the function F(L) (Figure 4c) evidences the presence of a certain amount of taut-tie molecules bridging the crystals. At sufficiently high draw ratio, the ''long'' SCS form the RAP (Figure 6a). Thus, a smooth transition from folded crystals to defect fibrillar crystalline structure take place during the drawing process (Figure 6b). The smaller the amount of defect sites, the higher the strength of the fiber.

At the same time, as the amorphous regions in fibrillar crystallite disappear, further force drawing would not only increase the modulus and strength but could induce the chain breakage in straight macromolecules with worsening the mechanical properties. Figure 7 shows the SCS distributions in two fibers with different ultimate draw ratio, which were prepared from different reactor powders. The fiber that has the smaller draw ratio exhibits the higher strength. The LAM spectroscopy allows one to elucidate some

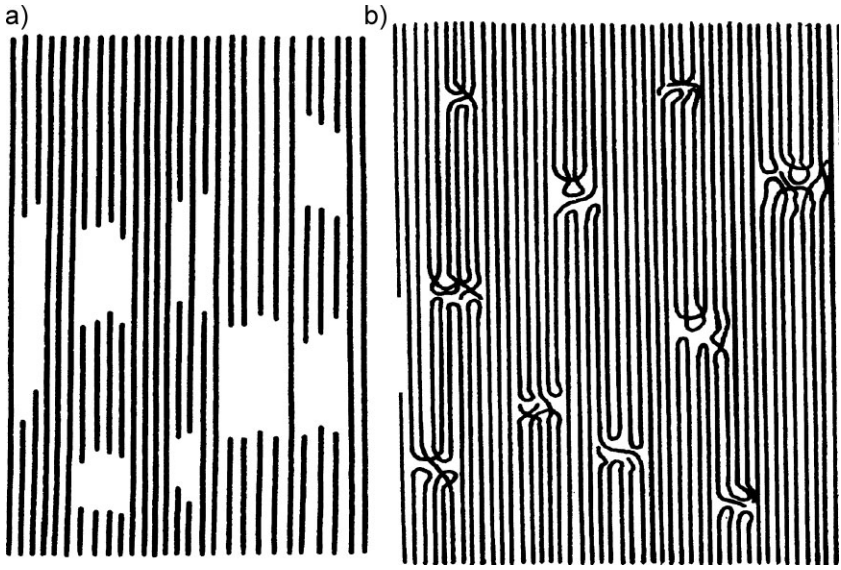

Figure 6.
Schematic representation of the bridging model of highly oriented polymer (a) and the associated model of the crystalline structure with the prevalence of ordered phase (b).

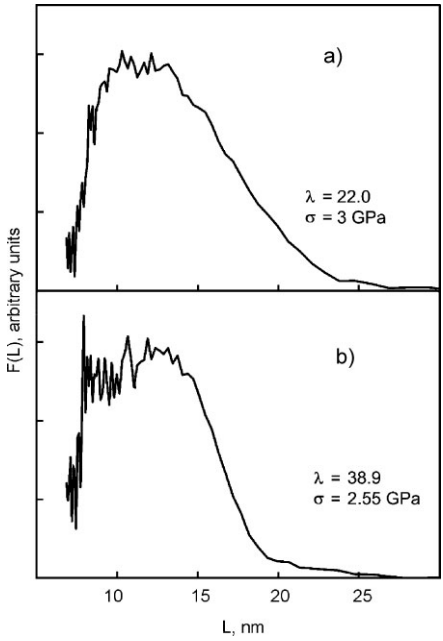

Figure 7.
The SCS length distributions in UHMWPE fibers characterized by different ultimate draw ratio and tensile strength. Two-stage drawing from the 3 wt.% solution in the paraffin oil was performed at the industry equipment[16].

important characteristics of the oriented structure, which could be related with the fibers strength. In Figure 7, one can see that the higher drawn sample is characterized by the actual lack of the fraction of ''long'' SCS, such as those with lengths 18–30 nm, which are present in the lower drawn sample. In addition, a peak at ~7 nm is seen in the SCS length distribution of the former one. These data evidence that the higher draw ratio was not due to by the extra straightening of molecular chains but due to breaking and slipping of the longest ones. The 7 nm peak belongs to the products of such breakage. These relatively short SCS incapable to carry a significant load what results in limited tensile strength of the fiber.

Reactor Powders

There are a number of experimental evidences that the mechanical performance of the final product depend, to a considerable degree, on properties of the initial polymeric raw, in particular, on the morphology of reactor powder – the advanced

substance which is used for manufacturing high-performance PE fibers.[17–23] At the same time, the role of morphology in forming fiber's mechanical properties remains, in many instances, unclear. In this work, two UHMWPE reactor powders synthesized under different conditions were characterized with the help of the low-frequency Raman spectroscopy and the scanning electron microscopy (SEM), and the elastic properties and strength of fibers prepared from these powders through the gel extrusion were compared. Some characteristic of the reactor powders synthesized under different conditions are given in Table 1 (columns 1 to 3).

The SEM images and the low-frequency Raman spectra of the samples are shown in Figure 8 and Figure 9, respectively. From putting in comparison Figure 8 and Figure 9 one can conclude that the SCS length distribution in the powder with a more consolidated morphology (sample B) exhibits a single peak at 17 nm. At the same time, a bimodal distribution takes place in powder A: its high-amplitude peak at 19 nm is supplemented with the feature at 32 nm. A comparison of these data with the results of mechanical tests of the fibers drawn from the reactor powders shows (Table 1, column 4 to 6) that the higher values of both the Young's modulus and tensile strength were achieved in fiber formed from the powder A that exhibits more tenuous morphology and has, correspondingly, the bimodal SCS length distribution. It was found previously[18] that the reactor powders with tighter morphology had much worse mechanical properties than the powders having low consolidated structure.

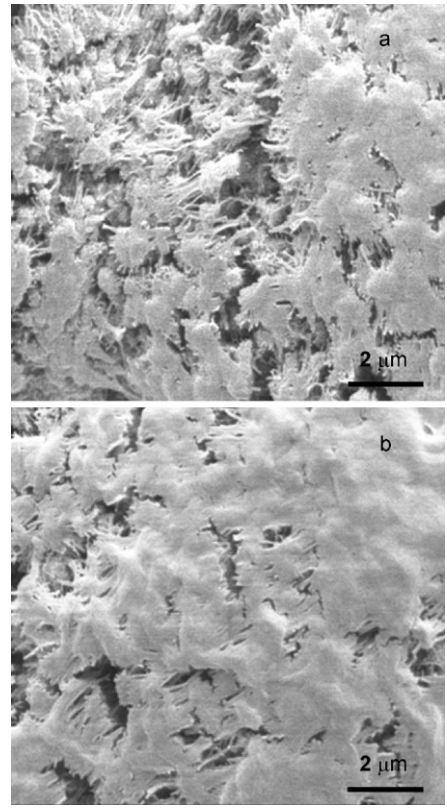

Figure 8.
SEM images of reactor powders characterized in Table 1. a – sample A; b – sample B.

Thus, the reactor powders that could be utilized for manufacturing high-strength UHMWPE fibers should contain a fraction of "long" SCS and have the low-consolidated morphology. Issuing from this conclusion, and having found the optimal conditions of the extrusion-drawing procedures, we for the first time succeeded to obtain the UHMWPE filament with the tensile strength 4 GPa using the industry equipment [24].

Table 1.
Characteristics of reactor powders and fibers prepared from them under the same conditions.

Sample	Powder		Fiber		
	Polymerization temperature, °C	$M_W^* \times 10^6$ g/mol	Ultimate draw ratio	Young's modulus, GPa	Tensile strength, GPa
A	52	3.6	20	98	3.00
B	55	2.7	39	94	2.55

*Viscosity-average molecular weight.

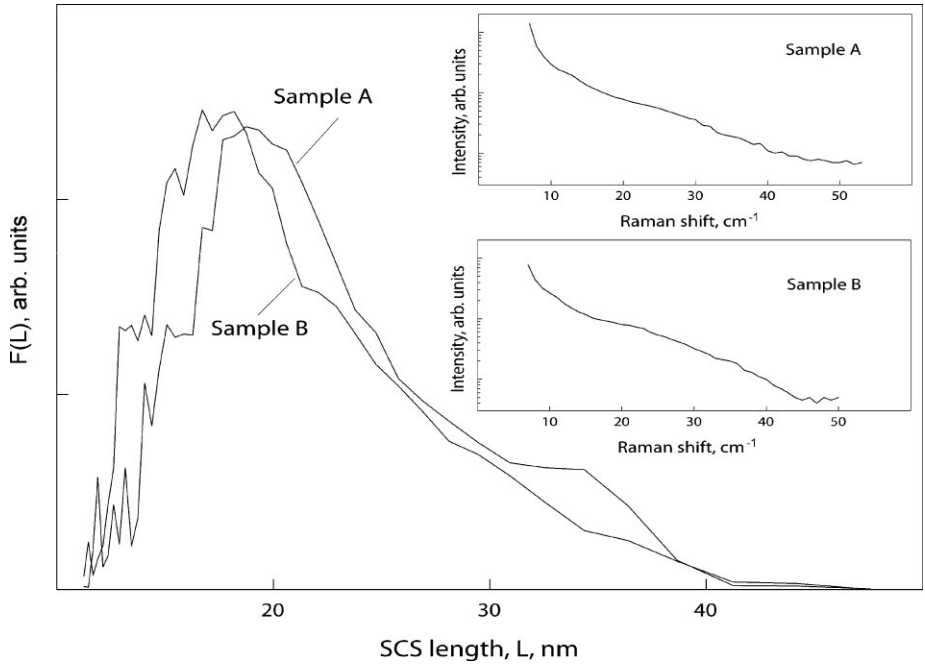

Figure 9.
Low-frequency Raman spectra (cut-ins) and calculated from them SCS length distributions in reactor powders characterized in Table 1.

Conclusion

The low-frequency Raman spectroscopy gives information on the ordered structures in semi-crystalline polymers taken in the form of powders, gels, or oriented fibers. The presented results demonstrate that the straight chain segments existing in non-oriented polymeric substances, which serve as raw materials for manufacturing highly-drawn fibers, could affect the fibers' mechanical properties through either limiting or promoting the formation of optimal molecular network to be transformed into the highly oriented structure.

[1] R. F. Schaufele, T. Schimanouchi, *J. Chem. Phys.* **1967**, *47*, 3605.
[2] R. G. Snyder, S. J. Krause, J. R. Scherer, *J. Polym. Sci.: Polym. Phys. Ed.* **1978**, *16*, 1593.
[3] G. Capaccio, M. A. Wilding, I. M. Ward, *J. Polym. Sci.: Polym. Phys. Ed.* **1981**, *19*, 1489.
[4] P. M. Pakhomov, "*High-strength Polymer Fibers*", Tver State Univ., Tver **1993**, p. 4.
[5] P.-G. De Gennes, *Scaling Concepts in Polymer Physics*, Cornell Univ. Press, Ithaca and London **1978**, p. 142.
[6] A. Keller, *Faraday Discass.* **1996**, *101*, 1.
[7] P. Pakhomov, A. Tshmel, S. Khizhnyak, V. Galitsyn, *Doklady AN (Russia)* **2002**, *386*, 220.
[8] K. Kober, S. Khizhnyak, P. Pakhomov, A. Tshmel, *J. Appl. Polym. Sci.* **1999**, *72*, 1795.
[9] P. Pakhomov, S. Khizhnyak, K. Kober, A. Tshmel, *Europ. Polym. J.* **2001**, *37*, 623.
[10] P. Pakhomov, S. Khizhnyak, V. Galitsyn, A. Tshmel, *J. Macromol. Sci. -Phys.* **2002**, *B41*, 229.
[11] P. Pakhomov, S. Khizhnyak, H. Reuter, A. Tshmel, *J. Appl. Polym. Sci.* **2003**, *89*, 373.
[12] P. Barham, A. Keller, *J. Mater. Sci.* **1976**, *11*, 27.
[13] V. Galitsyn, S. Khizhnyak, P. Pakhomov, A. Tshmel, *J. Macromol. Sci. -Phys.* **2003**, *B42*, 1085.
[14] G. Capaccio, M. A. Wilding, I. M. Ward, *J. Polym. Sci.: Polym. Phys. Ed.* **1981**, *19*, 1489.
[15] M. Al-Hassian, G. R. Devies, I. M. Ward, *Polymer* **2001**, *42*, 3679.
[16] V. P. Galitsyn, V. P. Napasnikov, A. E. Mikushev, *RF Patent* No. 1796689, **1993**.

[17] K. Tsobkallo, V. Vasilieva, M. Kakiage, H. Uehara, A. Tshmel, *J Macromol. Sci. -Phys.* **2006**, *B45*, 407.
[18] P. Pakhomov, S. Khizhnyak, V. Galitsyn, B. Hartmann, B. Moeller, V. Nikitin, V. Zakharov, A. Tshmel, *J. Macromol. Sci. -Phys.* **2008**, *B47*, 1096.
[19] Y. M. T. Tervoort, P. J. Lemstra, *Polym. Commun* **1991**, *32*, 343.
[20] S. Ottani, E. Ferrecini, A. Ferrero, V. Malta, R. S. Porter, *Macromolecules* **1995**, *28*, 2411.
[21] H. Uehara, M. Nakae, T. Kanamoto et al. *Polymer* **1998**, *39*, 6127.
[22] Y. L. Joo, O. H. Han, H.-K. Lee, J. K. Song, *Polymer* **2000**, *41*, 1355.
[23] A. Sano, Y. Iwanami, K. Matsaura, S. Yokoyama, T. Kanamoto, *Polymer* **2001**, *42*, 5859.
[24] P. Pakhomov, V. Galitsyn, A. Krylov, S. Khizhnyak, A. Golikova, A. Tshmel, *Fibre Chemistry* **2005**, *37*, 319.

